

COORDINATION CONTROL OF STATE ERROR PCH AND RBFNN ADAPTIVE CONTROL FOR SPMSM DRIVE SYSTEM

YANG ZHAO¹, MINGLING SHAO², HAISHENG YU² AND JINPENG YU²

¹Editorial Office of Journal

²College of Automation Engineering

Qingdao University

No. 308, Ningxia Road, Qingdao 266071, P. R. China

yu.hs@163.com

Received June 2015; accepted August 2015

ABSTRACT. *In this paper, the coordination control model of surface permanent magnet synchronous motor (SPMSM) position drive system is systematically established based on the principle of signal and energy. The signal controllers are designed by proportional integral (PI) control and radial basis function neural network (RBFNN) direct model reference adaptive control (MRAC), which guarantee the fast position tracking control. The energy controllers are developed with port-controlled Hamiltonian (PCH) system, which achieve the real-time optimization control of input energy and output energy. The coordination control strategy is proposed based on the compound control of signal and energy. To illustrate the performance of the proposed controllers, simulations are implemented based on the designed scheme.*

Keywords: Surface permanent magnet synchronous motor, RBFNN direct MRAC, State error PCH, Position control

1. Introduction. Surface permanent magnet synchronous motors (SPMSMs) are widely used in high-precision servo systems. Among the various control methods, the control objective of SPMSM system based on signal control is to quickly eliminate the system error [1]. Furthermore, the control objective of SPMSM system based on energy control is to minimize loss energy and optimize the input energy and output energy [2].

The signal control possesses the advantages of rapid adjustment ability and fine dynamic response. Moreover, the neural network (NN) control is independent on the mathematical model [3]. In this paper, proportional integral (PI) control and radial basis function neural network (RBFNN) direct model reference adaptive control (MRAC) are studied to design the signal controllers [4]. By online adjusting the weight of RBFNN, the proposed controllers ensure strong robustness in the system. As the inertia link exists in the SPMSM system, a new error function is proposed to improve the control performance. In recent years, many research results of port-controlled Hamiltonian (PCH) system have been obtained since it has certain superiorities [5,6]. The state error PCH controllers of SPMSM are established as the energy controllers.

According to the above analysis, the coordination control strategy based on the compound control of signal and energy is presented to realize the position tracking control. Both signal controllers and energy controllers are adopted during the whole control process. The simulation results show that the system has rapid dynamic and steady state response, which demonstrate the feasibility and superiority of the proposed control method.

The remainder of the paper is organized as follows. The model of SPMSM drive system is described in Section 2. Then the position control principle is introduced in Section 3. And the controllers are developed in Section 4. The simulation results are given in Section 5. Finally, some conclusions are presented.

2. Modeling of SPMSM Drive System. The mathematical model of SPMSM drive can be described by the following equations [6]

$$\begin{cases} L_d di_d/dt = -R_s i_d + n_p \omega L_q i_q + u_d \\ L_q di_q/dt = -R_s i_q - n_p \omega L_d i_d - n_p \omega \Phi + u_q \\ J d\omega/dt = \tau - \tau_L = n_p [(L_d - L_q) i_d i_q + \Phi i_q] - \tau_L \\ d\theta/dt = \omega \end{cases} \quad (1)$$

$$\tau = n_p [(L_d - L_q) i_d i_q + \Phi i_q] \quad (2)$$

where R_s is the stator resistance, and Φ is the rotor flux linking the stator, respectively. The J is the moment of inertia, and n_p is the number of pole pairs, respectively. The ω and θ are mechanical angular speed and position of rotor, respectively. The τ and τ_L are electromagnetic and load torque, respectively.

3. Position Control Principle of SPMSM. The control objective of the SPMSM drive system is the tracking of the θ to the desired position θ_0 . To use the advantages of the signal control and energy control, the control scheme is presented in Figure 1. In Figure 1, the subscripts s and e represent the signal control and energy control, respectively. The RBFNN direct MRAC control and PI control are presented to get the u_{sd} and u_{sq} in the signal controllers. The u_{ed} and u_{eq} are obtained by the state error PCH control and $i_d^* = 0$ vector control with the known load torque in the energy controllers.

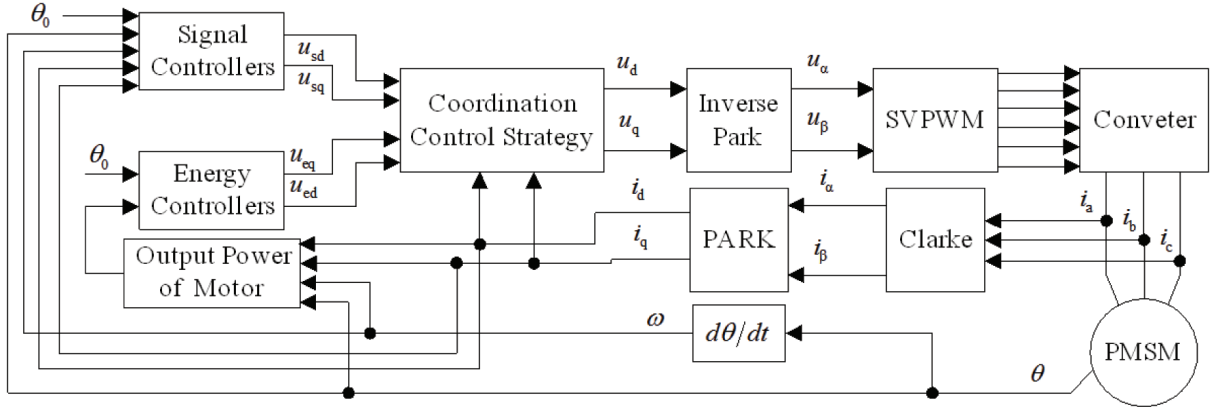


FIGURE 1. Block diagram of SPMSM drive system with signal and energy

4. Controllers Design of SPMSM System.

4.1. Design of signal controllers. The fast position tracking control is achieved based on the signal control. Signal controllers are composed of position controller, speed controller, d -axes current controller and q -axes current controller.

(1) Position controller design. Assuming θ , $\dot{\theta}$, ω , i_{sd} and i_{sq} are measurable signals. Let θ_r be the output of reference model. Equation (1) can be written into $a_1 \dot{\theta} + a_0 \theta = \omega$, where $a_1 = 1$ and $a_0 = 0$. Thus, the reference model can be chosen as $b_1 \dot{\theta}_r + b_0 \theta_r = \theta_0$ [7]. Consequently, the pulse transfer function can be gotten as $G_s(z) = \frac{1}{b_1} \frac{z}{z - e^{-b_0 T/b_1}}$, where $\theta_r(t) = (1/b_1) e^{-b_0 t/b_1} \theta_0$ can be obtained and T is sampling time.

As the inertia link exists in the SPMSM system, thus the error function is chosen as $E_s = e_s^2/2 = [(\theta_r - \theta) + kd(\dot{\theta}_r - \dot{\theta})]^2/2$ and kd is variable differential coefficient [8]. Figure 2 shows the structure of the proposed controller.

The input vector of RBFNN controller is expressed as $X = [x_1 \ \cdots \ x_m]$. And h_j is the Gaussian function. The weight matrix is $\mathbf{W} = [w_1 \ w_2 \ \cdots \ w_j \ \cdots \ w_m]$. The

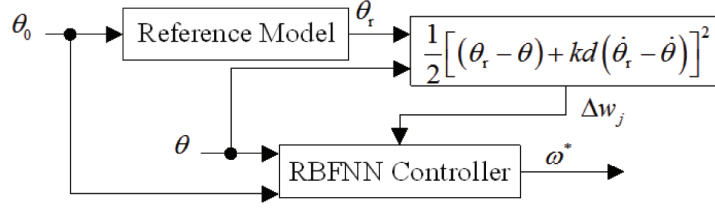


FIGURE 2. Simplified diagram of RBFNN direct MRAC controller

output of RBFNN can be written as $\omega^*(k) = h_1 w_1 + \dots + h_j w_j + \dots + h_m w_m$. The control target is that the error function $E_s = \frac{1}{2} e_s^2$ converges to zero by adjusting the weight. The control algorithm can be described as

$$\begin{cases} \Delta w_j(k) = -\eta \partial E_s(k) / \partial w_j = \eta e_s(k) (\partial \theta / \partial \omega^* + kd \partial \dot{\theta} / \partial \omega^*) h_j \\ w_j(k) = w_j(k-1) + \Delta w_j(k) + \alpha \Delta w_j(k) \end{cases} \quad (3)$$

where η is the learning rate and α is the momentum factor. In the SPMSM system, the exact value of $(\partial \theta / \partial \omega^* + kd \partial \dot{\theta} / \partial \omega^*)$ cannot be gotten as the motor model is inaccurate. Thus, $\text{sgn}(\partial \theta / \partial \omega^* + kd \partial \dot{\theta} / \partial \omega^*)$ can be chosen to replace $(\partial \theta / \partial \omega^* + kd \partial \dot{\theta} / \partial \omega^*)$.

(2) Speed controller design. The speed controller is designed according to PI control

$$i_{sq}^* = K_{p1}(\omega^* - \omega) + K_{i1} \int_0^t (\omega^* - \omega) dt \quad (4)$$

where K_{p1} is proportion coefficient and K_{i1} is integral coefficient, respectively.

(3) Current controllers design. The d -axes current controller is studied based on $i_d^* = 0$ and PI control, and PI control is proposed for q -axes current controller.

$$\begin{cases} u_{sd}^* = K_{p2}(i_d^* - i_d) + K_{i2} \int_0^t (i_d^* - i_d) dt \\ u_{sq}^* = K_{p3}(i_{sq}^* - i_{sq}) + K_{i3} \int_0^t (i_{sq}^* - i_{sq}) dt \end{cases} \quad (5)$$

where K_{p2} is proportion coefficient and K_{i2} is integral coefficient of d -axes current controller, respectively, K_{p3} is proportion coefficient and K_{i3} is integral coefficient of q -axes current controller, respectively.

(4) Stability analysis of SPMSM system. Define the Lyapunov function as $V_s(k) = [(\theta_r - \theta) + kd(\dot{\theta}_r - \dot{\theta})]^2 / 2$. The variation of $V_s(k)$ is $\Delta V_s(k) = [\Delta e_s(k)^2 + 2e_s(k)\Delta e_s(k)] / 2$, and the variation of $e_s(k)$ is $\Delta e_s(k) = e_s(k+1) - e_s(k) = \Delta \mathbf{W}(k) [\partial e_s(k) / \partial \mathbf{W}(k)]^T$. According to the RBFNN control algorithm

$$\Delta \mathbf{W}(k) = -\eta \frac{\partial E_s}{\partial \mathbf{W}(k)} = -e_s(k) \eta \frac{\partial e_s(k)}{\partial \mathbf{W}(k)} = e_s(k) \eta \text{sgn} \left(\partial \theta / \partial \omega^* + kd \partial \dot{\theta} / \partial \omega^* \right) \frac{\partial \omega^*}{\partial \mathbf{W}} \quad (6)$$

Let $\mathbf{A} = \partial e_s(k) / \partial \mathbf{W}(k)$ and $\Delta e_s(k) = -\eta \mathbf{A} \mathbf{A}^T e_s(k)$. Substituting $\Delta e_s(k)$ into $\Delta V_s(k)$ can get

$$\Delta V_s(k) = -e_s^2(k) (\mathbf{A} \mathbf{A}^T) [2\eta - \eta^2 (\mathbf{A} \mathbf{A}^T)] / 2 \quad (7)$$

When $0 < \eta < 2 (\mathbf{A} \mathbf{A}^T)^{-1}$, $\Delta V_s(k)$ is negative definite. The $V_s(k)$ is positive definite. Applying Lyapunov stability theorem, the system is stable.

4.2. Design of energy controllers. The optimization control of input energy and output energy is achieved via the state error PCH control.

According to Equations (1) and (2), the state vector, input vector and output vector of the SPMSM drive system are defined as follows

$$\begin{cases} \mathbf{x} = [x_1 \ x_2 \ x_3 \ x_4]^T = [L_d i_{ed} \ L_q i_{eq} \ J\omega \ \theta]^T \\ \mathbf{u}_e = [u_{ed} \ u_{eq}]^T, \quad \mathbf{i}_e = [i_{ed} \ i_{eq}]^T \end{cases} \quad (8)$$

$H(\mathbf{x})$ is the Hamiltonian function which equals the total stored energy of the system, that is

$$H(\mathbf{x}) = [x_1^2/L_d + x_2^2/L_q + x_3^2/J] / 2 + \tau_L x_4 \quad (9)$$

The models of PCH system with dissipation can be described as follows

$$\dot{\mathbf{x}} = [\mathbf{J}(\mathbf{x}) - \mathbf{R}(\mathbf{x})]\partial H(\mathbf{x})/\partial \mathbf{x} + \mathbf{g}(\mathbf{x})\mathbf{u}_e \quad (10)$$

The damping matrix $\mathbf{R}(\mathbf{x}) = \mathbf{R}^T(\mathbf{x}) \geq 0$ represents the dissipation. The interconnection structure is captured in matrix $\mathbf{g}(\mathbf{x})$ and skew-symmetric $\mathbf{J}(\mathbf{x}) = -\mathbf{J}^T(\mathbf{x})$. Equation (1) can then be rewritten in the PCH system form (10) with

$$\left\{ \begin{array}{l} \mathbf{J}(\mathbf{x}) = \begin{bmatrix} 0 & 0 & n_p x_2 & 0 \\ 0 & 0 & -n_p(x_1 + \Phi) & 0 \\ -n_p x_2 & n_p(x_1 + \Phi) & 0 & -1 \\ 0 & 0 & 1 & 0 \end{bmatrix} \\ \mathbf{g}(\mathbf{x}) = \begin{bmatrix} 1 & 0 \\ 0 & 1 \\ 0 & 0 \\ 0 & 0 \end{bmatrix}, \quad \mathbf{R}(\mathbf{x}) = \begin{bmatrix} R_s & 0 & 0 & 0 \\ 0 & R_s & 0 & 0 \\ 0 & 0 & 0 & 0 \\ 0 & 0 & 0 & 0 \end{bmatrix} \end{array} \right. \quad (11)$$

Considering the PCH system (10), given $H(\mathbf{x})$, $\mathbf{J}(\mathbf{x})$, $\mathbf{R}(\mathbf{x})$ and $\mathbf{g}(\mathbf{x})$, let \mathbf{x}_0 be a desired equilibrium and define $\tilde{\mathbf{x}} = \mathbf{x} - \mathbf{x}_0$ as the state error. Assign a closed-loop system desired energy function $H_d(\tilde{\mathbf{x}}) > 0$ and $H_d(0) = 0$.

If $\mathbf{J}_d(\tilde{\mathbf{x}}) = \mathbf{J}(\tilde{\mathbf{x}}) + \mathbf{J}_a = -\mathbf{J}_d^T(\tilde{\mathbf{x}})$ and $\mathbf{R}_d(\tilde{\mathbf{x}}) = \mathbf{R}(\tilde{\mathbf{x}}) + \mathbf{R}_a = \mathbf{R}_d^T(\tilde{\mathbf{x}}) \geq 0$ can be satisfied, feedback control $\mathbf{u} = \boldsymbol{\alpha}(\mathbf{x})$ can be found to satisfy

$$\begin{aligned} \mathbf{g}(\mathbf{x})\boldsymbol{\alpha}(\mathbf{x}) = & -[\mathbf{J}(\tilde{\mathbf{x}}) - \mathbf{R}(\mathbf{x})][\partial H(\mathbf{x})/\partial \mathbf{x} - \partial H_d(\tilde{\mathbf{x}})/\partial \tilde{\mathbf{x}}] - \mathbf{R}(\mathbf{x})\partial H(\mathbf{x})/\partial \mathbf{x}|_{\mathbf{x}=\mathbf{x}_0} \\ & - \mathbf{J}(\mathbf{x}_0)[\partial H(\mathbf{x})/\partial \mathbf{x} - \partial H(\mathbf{x})/\partial \tilde{\mathbf{x}}|_{\mathbf{x}=\mathbf{x}_0}] + [\mathbf{J}_a - \mathbf{R}_a]\partial H_d(\tilde{\mathbf{x}})/\partial \tilde{\mathbf{x}} + \mathbf{g}(\mathbf{x}_0)\mathbf{u}_0 \end{aligned} \quad (12)$$

The closed-loop PCH system (10) can be redescribed in the following form

$$\dot{\tilde{\mathbf{x}}} = [\mathbf{J}_d(\tilde{\mathbf{x}}) - \mathbf{R}_d(\tilde{\mathbf{x}})]\partial H_d(\tilde{\mathbf{x}})/\partial \tilde{\mathbf{x}} \quad (13)$$

The closed-loop system (13) will be asymptotically stable at the origin $\tilde{\mathbf{x}} = 0$ [9].

(1) Determination of equilibrium point for system. When the load torque is known, $\tau_L = \tau_{L0}$ can be obtained from Equation (1). Thus, from Equation (2)

$$\begin{cases} i_{ed0} = 0 \\ i_{eq0} = \tau_{L0}/n_p\Phi \end{cases} \quad (14)$$

The desired equilibrium state is selected as follows

$$\mathbf{x}_0 = [x_{10} \ x_{20} \ x_{30} \ x_{40}] = [L_d i_{ed0} \ L_q i_{eq0} \ J\omega_0 \ \theta_0] = [0 \ L_q \tau_{L0}/n_p\Phi \ J\omega_0 \ \theta_0] \quad (15)$$

At the equilibrium \mathbf{x}_0 , $L_d di_{ed}/dt = 0$ and $L_q di_{eq}/dt = 0$ are gotten. From Equation (1)

$$\mathbf{u}_{e0} = \begin{bmatrix} u_{ed0} \\ u_{eq0} \end{bmatrix} = \begin{bmatrix} R_s i_{ed0} - n_p L_q i_{eq0} \omega_0 \\ R_s i_{eq0} + n_p L_d i_{ed0} \omega_0 + n_p \Phi \omega_0 \end{bmatrix} \quad (16)$$

(2) Design of controller with the known load torque. The desired Hamiltonian function of the system is designed by

$$H_d(\tilde{\mathbf{x}}) = [\tilde{x}_1^2/L_d + \tilde{x}_2^2/L_q + \tilde{x}_3^2/J + \rho \tilde{x}_4^2]/2 \quad (17)$$

$\mathbf{J}_a(\mathbf{x})$ and \mathbf{R}_a can be taken as follows

$$\mathbf{J}_a(\mathbf{x}) = \begin{bmatrix} 0 & k_0 & -n_p \tilde{x}_2 & -L_d \tilde{x}_2 \\ -k_0 & 0 & n_p \tilde{x}_1 & L_q \tilde{x}_1 \\ n_p \tilde{x}_2 & n_p \tilde{x}_1 & 0 & 0 \\ L_d \tilde{x}_2 & L_q \tilde{x}_1 & 0 & 0 \end{bmatrix}, \quad \mathbf{R}_a = \begin{bmatrix} r & 0 & 0 & 0 \\ 0 & r & 0 & 0 \\ 0 & 0 & r_m & 0 \\ 0 & 0 & 0 & 0 \end{bmatrix} \quad (18)$$

where k_0 , r and r_m are interconnection and damping parameters to be designed, respectively. Substituting Equations (11), (14), (16)-(18) into (12), controllers of the system can be gotten as

$$u_{ed} = R_s i_{ed0} - r(i_{ed} - i_{ed0}) + k_0(i_{eq} - i_{eq0}) - \rho L_d L_q (i_{eq} - i_{eq0})(\theta - \theta_0) - n_p L_q i_{eq} \omega_e \quad (19)$$

$$u_{eq} = R_s i_{eq0} - k_0(i_{ed} - i_{ed0}) - r(i_{eq} - i_{eq0}) + \rho L_d L_q (i_{ed} - i_{ed0})(\theta - \theta_0) + n_p L_d i_{ed} \omega_e + n_p \Phi \omega_{e0} \quad (20)$$

Thus, the matching equation $\tau - \tau_L = -r_m(x_4 - x_{40})/J - \rho(x_3 - x_{30})$ shows that the mechanical subsystem is stable [9].

4.3. Design of coordination control strategy. In this paper, the coefficients in the index function form are designed to realize the smooth transition. Define $c_{sd}(t) \in [0, 1]$ and $c_{ed}(t) \in [0, 1]$ as the coefficient function of d -axis signal controller and d -axis energy controller, respectively. Set $c_{sq}(t) \in [0, 1]$ and $c_{eq}(t) \in [0, 1]$ as the coefficient function of q -axis signal controller and q -axis energy controller, respectively. Coefficient functions can be expressed as

$$\begin{cases} c_{sd}(t) = e^{-kt} \\ c_{ed}(t) = 1 - e^{-kt} \end{cases}, \quad \begin{cases} c_{sq}(t) = e^{-kt} \\ c_{eq}(t) = 1 - e^{-kt} \end{cases} \quad (21)$$

where k is taken from the actual situation. Then the coordination control strategy is

$$\begin{cases} u_d = c_{sd}(t) \cdot u_{sd} + c_{ed}(t) \cdot u_{ed} \\ u_q = c_{sq}(t) \cdot u_{sq} + c_{eq}(t) \cdot u_{eq} \end{cases} \quad (22)$$

5. Simulation Results. The simulations are performed to evaluate the performance of closed-loop system by using MATLAB/Simulink. The motor parameters are as follows. $R_s = 2.875\Omega$, $L_d = L_q = 8.5\text{mH}$, $\Phi = 0.175\text{Wb}$, $J = 0.02\text{kg} \cdot \text{m}^2$, $n_p = 4$. At $t = 0\text{s}$, the rotor given position is $\theta_0 = 45\text{rad}$, and the simulation time is 2.0s . The given load torque τ_{L0} changes from $3\text{N} \cdot \text{m}$ to $6\text{N} \cdot \text{m}$ at $t = 1.4\text{s}$.

Figure 3 is the position response curve based on the signal and energy control with $k = 5$, $k = 10$ and $k = 40$. It can be seen that the system can achieve the precise position control. Figure 4 represents the speed response curves with $k = 5$, $k = 10$ and $k = 40$. Figure 5 and Figure 6 represent the stator current response and the electromagnetic torque response curve with $k = 5$, respectively. The value of electromagnetic torque and stator current change rapidly during the starting stage of motor. In order to prevent the position overshoot, speed decreases rapidly when the position signal reaches the reference value.

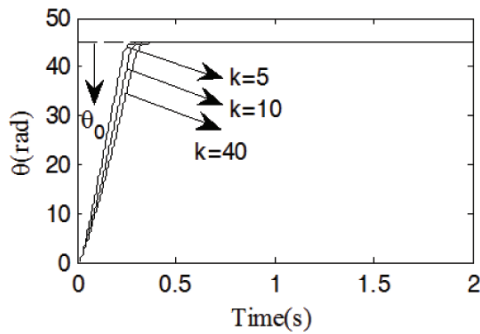


FIGURE 3. Position curve

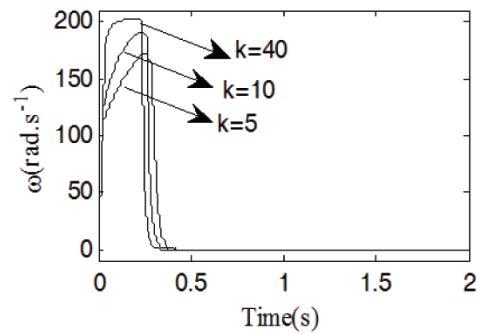


FIGURE 4. Speed curve

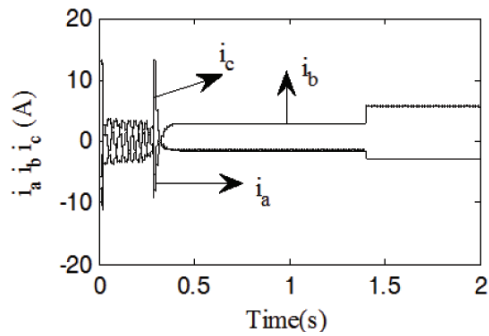


FIGURE 5. Stator current curve

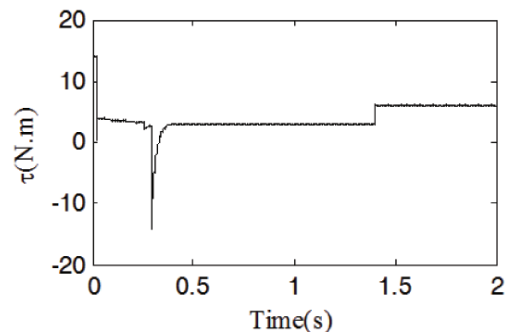


FIGURE 6. Electromagnetic torque curve

6. Conclusions. In this paper, the compound control based on signal and energy is proposed for the SPMSM drive system. Signal controllers are designed based on the RBFNN direct MRAC control and PI control. The state error PCH controllers are employed as the energy controllers. SPMSM drive system realizes the position tracking control, fast dynamic and steady state response through the signal control. Furthermore, the real-time optimization control of input energy and output energy is achieved by the energy control in the SPMSM system. By reducing the total input energy and improving the output energy, the system has minimum total energy loss. The system simulation results demonstrate the advantages of the designed coordination control strategy, which show that the controllers based on the coordination control strategy improve the dynamic and steady state performances. In the future work, the presented scheme will be realized by DSP2812.

Acknowledgement. This work is supported by the National Natural Science Foundation of China (61573203, 61573204) and Shandong Province Outstanding Youth Foundation (ZR2015JL022).

REFERENCES

- [1] M. Morawiec, The adaptive backstepping control of permanent magnet synchronous motor supplied by current source inverter, *IEEE Trans. Industrial Informatics*, vol.9, no.2, pp.1047-1055, 2013.
- [2] H. Yu, J. Yu, J. Liu and Y. Wang, Energy-shaping and L2 gain disturbance attenuation control of induction motor, *International Journal of Innovative Computing, Information and Control*, vol.8, no.7(B), pp.5011-5024, 2012.
- [3] F. F. M. El-Sousy, Intelligent optimal recurrent wavelet Elman neural network control system for permanent-magnet synchronous motor servo drive, *IEEE Trans. Industrial Informatics*, vol.9, no.4, pp.1986-2003, 2013.
- [4] C. Xia, W. Qi, R. Yang and T. Shi, Identification and model reference adaptive control for ultrasonic motor based on RBF neural network, *Proc. of the CSEE*, vol.24, no.7, pp.117-121, 2004.
- [5] R. Ortega, A. van der Schaft, B. Maschke and G. Escobar, Interconnection and damping assignment passivity-based control of port-controlled Hamiltonian systems, *Automatica*, vol.38, pp.585-596, 2002.
- [6] H. Yu, J. Yu and Y. Wang, Energy-shaping control of PMSM based on maximum output power and load torque observer, *ICIC Express Letters*, vol.7, no.1, pp.241-246, 2013.
- [7] C. Gao, Y. Shen and Z. Ji, Model reference fuzzy adaptive control of permanent magnet synchronous motor, *Journal of System Simulation*, vol.20, no.7, pp.1817-1820, 2008.
- [8] H. Yu, J. Yu, N. Zhu and Q. Wei, Speed regulation of permanent magnet synchronous motor based on neuron adaptive control, *ICIC Express Letters, Part B: Applications*, vol.4, no.3, pp.565-571, 2013.
- [9] H. Yu, J. Yu, J. Liu and Q. Song, Nonlinear control of induction motors based on state error PCH and energy-shaping principle, *Nonlinear Dynamics*, vol.72, nos.1-2, pp.49-59, 2013.